CrossMark
click for updates

Genotypic Differences in Dengue Virus Neutralization Are Explained by a Single Amino Acid Mutation That Modulates Virus Breathing

Kimberly A. Dowd, Christina R. DeMaso, Theodore C. Pierson

Viral Pathogenesis Section, Laboratory of Viral Diseases, National Institute of Allergy and Infectious Diseases, National Institutes of Health, Bethesda, Maryland, USA

ABSTRACT Flaviviruses sample an ensemble of virion conformations resulting from the conformational flexibility of their structural proteins. To investigate how sequence variation among strains impacts virus breathing, we performed studies with the monoclonal antibody (MAb) E111, which binds an inaccessible domain III envelope (E) protein epitope of dengue virus serotype 1 (DENV1). Prior studies indicated that an observed ~200-fold difference in neutralization between the DENV1 strains Western Pacific-74 (West Pac-74) and 16007 could not be explained by differences in the affinity of MAb E111 for each strain. Through neutralization studies with wild-type and variant viruses carrying genes encoding reciprocal mutations at all 13 amino acid differences between the E proteins of West Pac-74 and 16007, we found that E111 neutralization susceptibility mapped solely to the presence of a lysine or arginine at E domain II residue 204, located distally from the E111 epitope. This same residue correlated with neutralization differences observed for MAbs specific for epitopes distinct from E111, suggesting that this amino acid dictates changes in the conformational ensembles sampled by the virus. Furthermore, an observed twofold difference in the stability of infectious West Pac-74 versus 16007 in solution also mapped to E residue 204. Our results demonstrate that neutralization susceptibility can be altered in an epitope-independent manner by natural strain variation that influences the structures sampled by DENV. That different conformational ensembles of flaviviruses may affect the landscape available for antibody binding, as well as virus stability, has important implications for functional studies of antibody potency, a critical aspect of vaccine development.

IMPORTANCE The global burden of dengue virus (DENV) is growing, with recent estimates of ~390 million human infections each year. Antibodies play a crucial role in protection from DENV infection, and vaccines that elicit a robust antibody response are being actively pursued. We report here the identification of a single amino acid residue in the envelope protein of DENV serotype 1 that results in global changes to virus structure and stability when it is changed. Our results indicate that naturally occurring variation at this particular site among virus strains impacts the ensemble of structures sampled by the virus, a process referred to as virus breathing. The finding that such limited and conservative sequence changes can modulate the landscape available for antibody binding has important implications for both vaccine development and the study of DENV-reactive antibodies.

Dengue virus (DENV) is a medically important flavivirus transmitted through the bite of an infected mosquito. An estimated 390 million human infections occur annually, with ~3.6 billion people living in areas where they are at risk (1). Flavivirus virions encapsidate a positive-sense, single-stranded, ~11-kb RNA genome. At least 10 viral proteins are translated from a single open reading frame, including the three structural proteins, capsid (C), premembrane/membrane (prM/M), and envelope (E) (2). Four antigenically related serotypes of DENV circulate in nature, and they vary by ~25 to 40% at the amino acid level. Each DENV serotype can be further classified into genotypes, which vary by ~6% and 3% at the nucleotide and amino acid levels, respectively (3, 4). For example, five distinct genotypes of DENV serotype 1 (DENV1) have been identified (5). Cryo-electron microscopy (Cryo-EM) reconstructions of mature DENV revealed a virion containing 180 E proteins arranged in rafts of three head-to-tail homodimers oriented roughly parallel to the surface (6, 7). In this configuration, the accessibility of an epitope for antibody recognition may differ as a function of its location on the virion (8, 9). E proteins are composed of three ectodomains (domains I, II, and III) and represent the major target of neutralizing antibodies (10). While the 75 amino acid M peptide is also present on the mature virion, its role in the biology of the virus and recognition by antibodies remains unknown.

The proteins of both enveloped and nonenveloped viruses explore multiple conformations at equilibrium (11). Thus, viruses exist as an ensemble of structures via a process called virus breathing. Virus structural dynamics was first inferred from neutralization studies of influenza virus and polioviruses that unexpectedly observed recognition of viral epitopes not predicted to be accessi-

ble on the surface of the virion (12, 13). For example, antibodies that bind the VP4 protein of poliovirus, a component of the virion located inside the capsid, inhibited infection in a time- and temperature-dependent manner (12). Similar patterns have now been reported for flaviviruses (14–16). Virus breathing varies the antigenic landscape for antibody binding, as epitopes may be differentially accessible for binding among members of a structural ensemble. Beyond changes in antibody recognition, virus breathing may play a role in the biology of virions. For example, small molecules that inhibit the dynamic motion of picornaviruses exert antiviral activity by preventing viral uncoating (17, 18). The interactions that govern the structural ensemble sampled by virions are unclear.

The existing structures of flaviviruses capture only a snapshot of the structural ensemble under defined experimental conditions. Detailed insight into the structures of flaviviruses under physiological conditions is experimentally challenging due to the structural heterogeneity associated with dynamic virions. For example, while the first solved DENV structure utilized virus produced in insect cells propagated at temperatures of $\leq 30°C$ (6), two recent studies reported that a brief incubation of DENV2 strains at 36 or 37°C revealed a heterogeneous population of virions, some of which possessed an increased diameter and bumpy appearance due to a reorganization of the E proteins (19, 20). It is interesting that not all DENV appear to adopt these alternative conformations; analogous studies with representative DENV1 and DENV4 strains observed relatively smooth viruses at this temperature (21). Thus, sequence variation may dictate the structural ensembles sampled by different virus strains.

Antibodies are sensitive tools to detect the dynamic properties of infectious virions because they have the ability to trap even transiently exposed epitopes. Furthermore, antibodies represent a critical component of immune protection against flavivirus infection (22). In order to understand immunity and inform the design of therapeutics and vaccines, numerous mouse and human monoclonal antibodies (MAbs) have been mapped and characterized *in vitro* and *in vivo*. Curiously, many of the epitopes recognized by neutralizing antibodies are not predicted to be accessible for recognition on the surface of the mature virion (9, 14, 23–27). E111 is a DENV1-specific MAb that binds a cryptic epitope in E domain III that is hypothesized to be exposed only via viral breathing (23, 28). The sensitivity of different DENV1 genotypes to E111 neutralization varies greatly. Recent studies demonstrated that the DENV1 genotype 2 strain 16007 was significantly more sensitive to E111 neutralization than the genotype 4 strain Western Pacific-74 (West Pac-74 [WP-74]) (23). Because the mode of E111 recognition was hypothesized to involve viral breathing, in the current study, we aimed to identify the precise amino acid residue(s) responsible for the differential sensitivity of these two closely related strains. Remarkably, our results identified a single amino acid within E (E-204) located ~54 Å from the crystallographically defined E111 epitope which was responsible for this genotypic difference in neutralization sensitivity. Our studies suggest that E-204 modulates the structural ensembles sampled by each virus, resulting in changes in the antigenic surface and in the overall stability of each virus in solution.

RESULTS

Amino acid variation in the E111 epitope does not explain the differential neutralization sensitivity of DENV1 strains 16007 and West Pac-74. Quantitative neutralization studies demonstrate that MAb E111 is markedly more efficient at inhibiting infection of the DENV1 strain 16007 compared to strain West Pac-74 (WP-74) (~175-fold difference in 50% effective concentration [EC$_{50}$]), as described previously (Fig. 1) (23, 28). Comparison of the E protein sequences of DENV strains 16007 and WP-74 revealed two amino acid residues (339 and 345) that differed among domain III (DIII) residues that comprise the E111 epitope (Table 1) (23). Surface plasmon resonance (SPR) binding assays of mutant and wild-type DIII variants identified a role for residue 345, but not residue 339, in the durability of E111 binding. However, this finding did not explain differences in neutralization sensitivity, as E111 neutralization studies revealed only a minimal role for residue 345 (23).

To extend these published findings, we generated DENV strain 16007 and WP-74 reporter virus particles (RVPs) incorporating reciprocal mutations at E residues 339 and 345, both individually and together. All six mutants were infectious, with titers within 1.5 log units of wild-type RVPs (data not shown). Antibody dose-response studies were performed, and the sensitivity of each variant to MAb E111 neutralization was compared to the sensitivity of the wild-type strain (Fig. 1). The presence of a serine (S) or threonine (T) at position 339 had no effect on E111 neutralization ($P = 0.996$ and $P = 0.250$ for the EC$_{50}$ values of wild-type strain WP-74 versus WP-74 S339T mutant and wild-type strain 16007 versus 16007 T339S mutant, respectively) (Fig. 1A and D). In agreement with prior results, the impact of a valine-to-alanine substitution at residue 345 (V345A) was not responsible for the large difference in neutralization sensitivity observed among these strains, although a modest (~2.6-fold) increase in neutralization of the WP-74 V345A mutant was observed compared to wild-type WP-74 ($P = 0.005$) (23). Interestingly, a change in neutralization susceptibility was not observed with the reciprocal 16007 A345V variant, which was as sensitive as the wild-type 16007 strain was ($P = 0.650$) (Fig. 1B and D). No significant difference in E111 neutralization was observed when both mutations were present ($P = 0.357$ and $P > 0.999$ for EC$_{50}$s of WP-74 versus WP-74 S339T/V345A and 16007 versus 16007 T339S/A345V, respectively) (Fig. 1C and D). Our results confirm that the amino acid differences located within the E111 epitope, whether expressed alone or together, cannot explain the large difference in E111 neutralization potency observed against strains 16007 and WP-74.

Identification of a single amino acid residue in E domain II that modulates E111 neutralization from a distance. To identify the molecular determinants for MAb E111 sensitivity, we expanded our analysis outside the crystallographically defined E111 epitope to include all amino acid differences between the E proteins of virus strains 16007 and WP-74. Sequence comparison identified 13 amino acid differences (including residues 339 and 345) (Table 1 and Fig. 2A). First, a panel of six DENV RVP variants was generated using E protein chimeras between strains 16007 and WP-74 (Fig. 2A and B). All these mutant RVPs were infectious, with titers within 1.2 log units of the wild-type RVP titer (data not shown). E111 neutralization experiments demonstrated that RVPs incorporating chimeric E proteins behaved similarly to either the wild-type 16007 or WP-74 RVPs (Fig. 2C to E). The mean
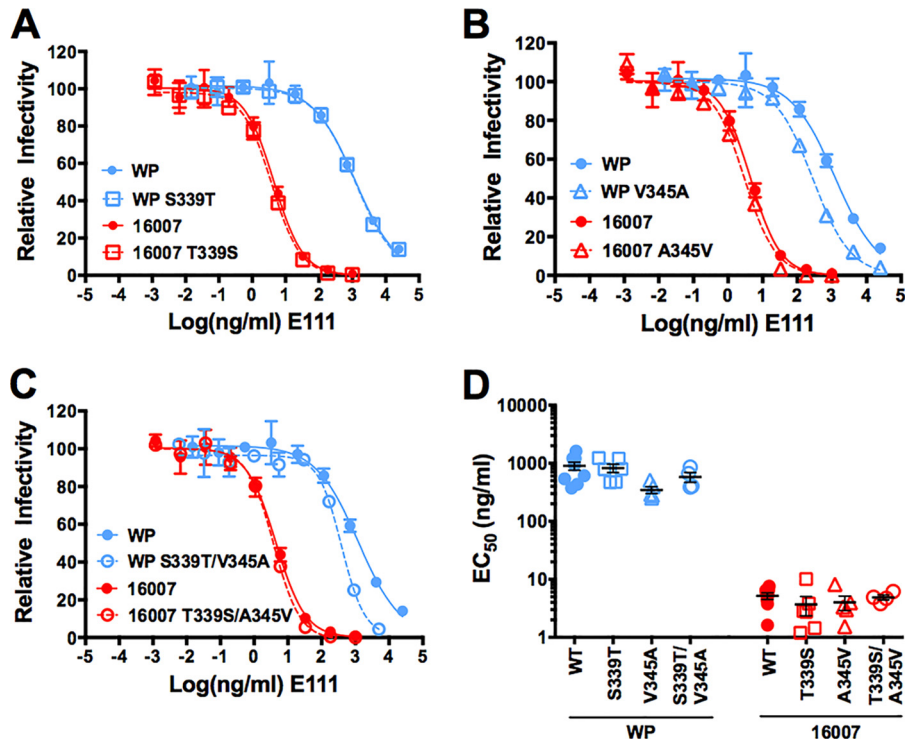
FIG 1 Amino acid differences in the E111 epitope are not responsible for the difference in neutralization between DENV1 strains 16007 and WP-74. Dose-response neutralization profiles were generated by incubating RVPs with serial dilutions of the MAb E111 for 1 h at 37°C, followed by addition of Raji-DCSIGNR cells. After 48 h, the number of infected, GFP-positive cells was determined by flow cytometry. The resulting data were fit by nonlinear regression (variable slope) to predict the EC_{50}. (A to C) Representative E111 neutralization profiles against wild-type (WT) 16007 and WP-74 (WP) RVPs compared to mutant RVPs expressing the reciprocal amino acids at E positions 339, 345, and 339 and 345 in combination, respectively. Error bars represent the range of duplicate infections. (D) EC_{50}s from four to nine independent experiments per RVP. Each symbol represents the value for an individual experiment. The means (short horizontal lines) ± standard errors (error bars) for the experiments are shown.

EC_{50} for each of the six chimeras was <4-fold different than EC_{50}s calculated for either WP-74 or 16007. While both WP-74 and 16007 chimeras 2 and 3 behaved similarly to their parental strain, analysis of neutralization curves and EC_{50}s identified two outliers: MAb E111 neutralization of WP-74 chimera 1 was similar to neutralization of wild-type 16007, whereas neutralization of 16007 chimera 1 was similar to neutralization of wild-type WP-74. Se-

TABLE 1 E protein amino acid differences between DENV1 strains 16007 and WP-74

Position[a]	Amino acid in virus strain:		Domain[b]
	WP-74	16007	
37	D	N	I
88	T	A	II
180	A	T	I
202	E	K	II
203	K	E	II
204	K	R	II
339	S	T	III
345	V	A	III
432	V	M	Stem
436	I	V	Stem
439	I	V	Stem
472	S	N	TM
478	T	M	TM

[a] Numbering from the start of the E protein.
[b] E protein domain. TM, transmembrane.

quence analysis of the E protein segment responsible for reversing this phenotype identified three contiguous residues located within E protein DII (E-DII) that differed between WP-74 and 16007 (residues 202, 203, and 204).

Next, an additional panel of 16007 and WP-74 RVP variants was generated with E proteins mutated to express single reciprocal amino acid variations at the remaining 11 E protein differences (residues 339 and 345 shown in Fig. 1) (Table 1 and Fig. 2A). All mutant RVPs were infectious, with titers within 1.2 log units of the RVP titers produced using wild-type structural proteins (data not shown). MAb E111 neutralization of mutant RVPs was assessed and compared to E111 neutralization of the wild-type strains (Fig. 3). Mutation of most of the amino acids that vary between strains WP-74 and 16007 resulted in no change compared to the parental wild-type strain (residues 37, 88, 180, 432, 436, 438, 472, and 478; $P \geq 0.854$) (Fig. 3A to C and G to L). These results are consistent with data obtained from studies of WP-74 and 16007 RVPs incorporating E protein chimeras (Fig. 2).

Analysis of MAb E111 neutralization results of structural gene chimera RVPs (Fig. 2) defined E protein residues 202, 203, and 204 as potential candidates of interest. Similar to the pattern observed with variants at position 345 (Fig. 1), mutation of residue 202 resulted in a small but significant threefold change in E111 neutralization susceptibility on the WP-74 background, but not the 16007 background ($P < 0.005$ and $P = 0.967$ for the EC_{50} values of WP-74 versus WP-74 E202K and 16007 versus 16007 K202E, re-
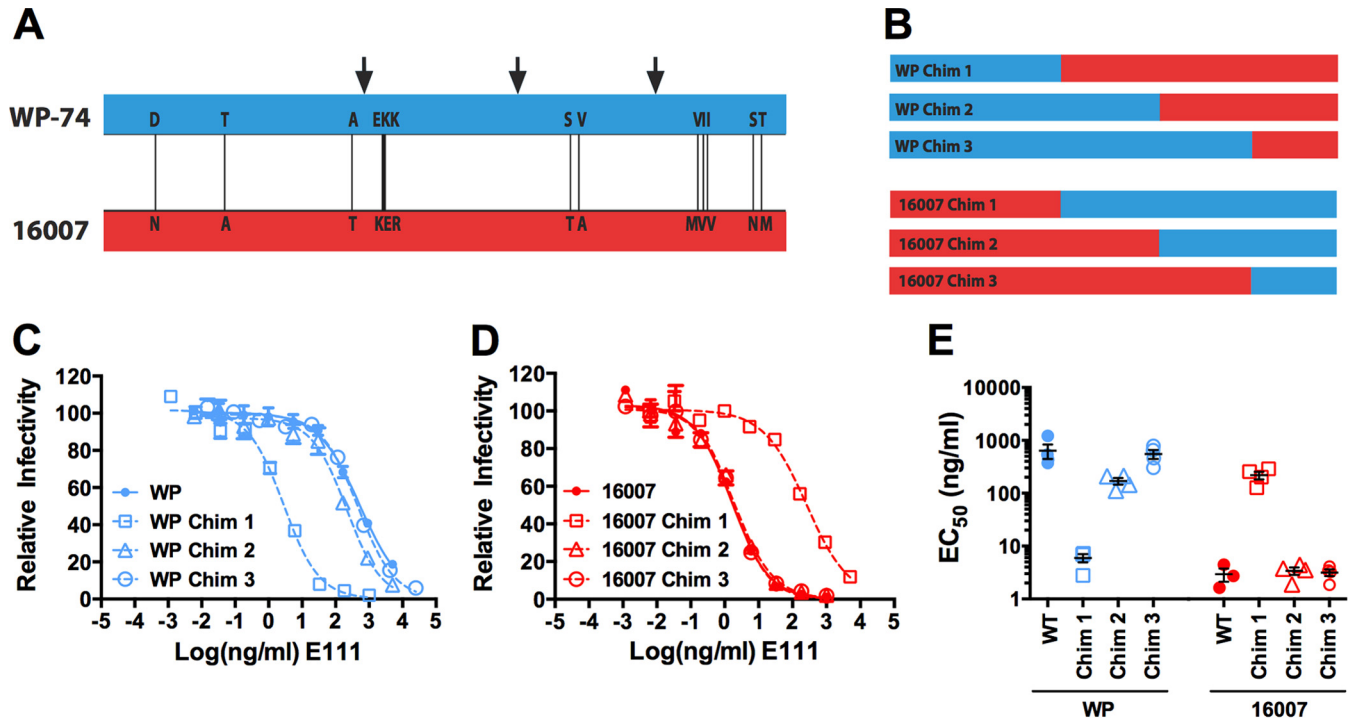
FIG 2 E111 neutralization of RVPs incorporating DENV strain 16007 and WP-74 E protein chimeras. (A) Schematic of the E proteins of DENV1 strains 16007 and WP-74. The vertical lines designate the locations of all 13 amino acid differences. The black arrows show the breakpoints used for cloning E protein chimeras. (B) Schematic of E protein chimeras used to generate RVPs. (C to E) Dose-response neutralization profiles were generated by incubating RVPs with serial dilutions of the MAb E111 for 1 h at 37°C, followed by addition of Raji-DCSIGNR cells. After 48 h, the number of infected, GFP-positive cells was determined by flow cytometry. The resulting data were fit by nonlinear regression (variable slope) to predict the EC_{50}. (C and D) Representative E111 neutralization profiles against wild-type 16007 and WP-74 RVPs compared to E protein chimera RVPs. The error bars represent the range of duplicate infections. (E) EC_{50}s from three or four independent experiments per RVP. Each symbol represents the value for an individual experiment. The means (short horizontal lines) ± standard errors (error bars) for the experiments are shown. Chim, Chimera; WP, WP-74; WT, wild type.

spectively) (Fig. 3D and L). Following this pattern, exchanging amino acids at residue 203 resulted in a significant 4.6-fold change in neutralization on the WP-74 background, but not the 16007 background ($P < 0.005$ and $P = 0.095$ for WP-74 versus WP-74 K203E and 16007 versus 16007 E203K EC_{50} values, respectively) (Fig. 3E and L). Despite these observations, when mutated individually, amino acids at residues 202 and 203 were clearly not the basis for the observed difference in E111 neutralization susceptibility. In contrast, introduction of the reciprocal amino acids at E-DII residue 204 essentially reversed the neutralization phenotype between WP-74 and 16007 strains ($P < 0.001$ for both WP-74 versus WP-74 K204R and 16007 versus 16007 R204K EC_{50}s) (Fig. 3F and L). The 175-fold difference in neutralization potency observed between strains WP-74 and 16007 was reduced to <5-fold when either strain was mutated to express the reciprocal amino acid present at residue 204. Remarkably, residue E-204 is located in DII, ~54 Å from the defined E111 epitope (Fig. 4).

Combined effects of E residues 202, 203, 204, and 345 on E111 neutralization. While the lysine versus arginine difference at residue 204 resulted in very large changes in MAb E111 neutralization potency, variation at E-204 did not entirely account for the neutralization phenotype observed for strains WP-74 and 16007. Because nearby mutations at residues 202 and 203 modestly altered E111 neutralization sensitivity (Fig. 3D, E, and L), we next investigated whether the introduction of combinations of these residues could fully recapitulate the patterns of neutralization ac-

tivity observed with wild-type strains. WP-74 K204R and 16007 R204K RVP constructs were additionally mutated to produce double mutants at residues 202 and 204 and residues 203 and 204, as well as triple mutants encoding the amino acid variation at residues 202, 203, and 204. All variants generated infectious titers within 1.5 log units of the wild-type RVP titer, with the exception of 16007 K202E/R204K, which had a 2.6-log-unit decrease in titer compared to the titer of wild-type 16007 (data not shown). E111 neutralization studies demonstrated that these combinations of mutations were not able to eliminate the <5-fold difference in EC_{50}s observed between wild-type and E-204 variant RVPs (Fig. 5). A small, but significant (1.9- to 7.2-fold) difference in neutralization potency between the variant and nearest wild-type construct was maintained ($P \leq 0.047$ for comparisons of variant to nonparental wild-type strain EC_{50}s) (Fig. 5B to E).

Variation at residue 345, located within the MAb E111 epitope, was responsible for a slight but significant impact on E111 neutralization potency (WP-74 V345A RVPs [Fig. 1B and D]). Additionally, alanine-to-valine substitution on the 16007 background resulted in decreased affinity of E111 binding to E-DIII constructs as determined by surface plasmon resonance studies (23). On the basis of these results, we additionally generated and characterized residue 204/345 double mutant RVPs for E111 neutralization sensitivity. Variant RVPs generated infectious titers within 1.2 log units of those of wild-type constructs (data not shown). E111 neutralization of residue 204/345 double mutant RVPs also did
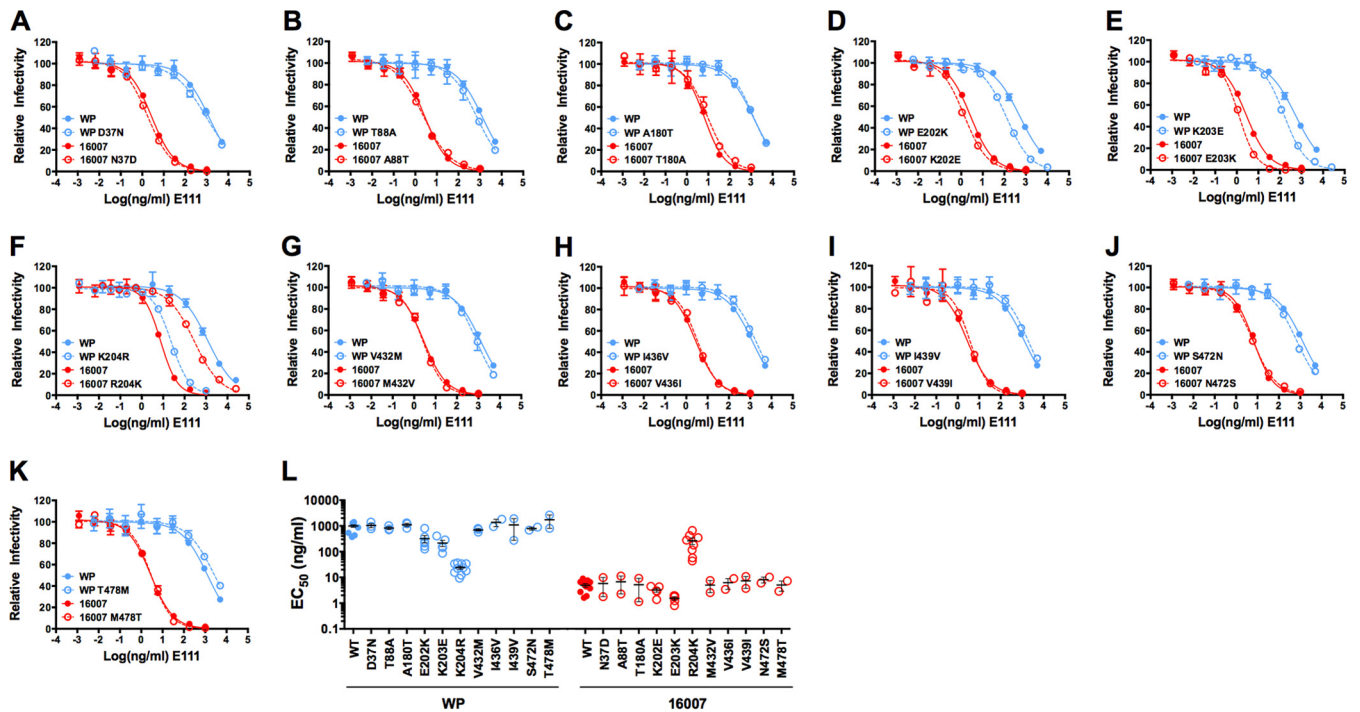
FIG 3 E111 neutralization of 16007 and WP-74 RVPs incorporating reciprocal E protein amino acid differences. Dose-response neutralization profiles were generated by incubating RVPs with serial dilutions of the MAb E111 for 1 h at 37°C, followed by addition of Raji-DCSIGNR cells. After 48 h, the number of infected, GFP-positive cells was determined by flow cytometry. The resulting data were fit by nonlinear regression (variable slope) to predict the EC_{50}. (A to K) Representative E111 neutralization profiles against wild-type (WT) 16007 and WP-74 (WP) RVPs compared to mutant RVPs encoding the reciprocal amino acids at E residues 37, 88, 180, 202, 203, 204, 432, 436, 439, 472, and 478, respectively. Error bars represent the range of duplicate infections. (L) EC_{50}s from 2 to 11 independent experiments per RVP. The horizontal line and error bars represent the mean and range or standard error, respectively.
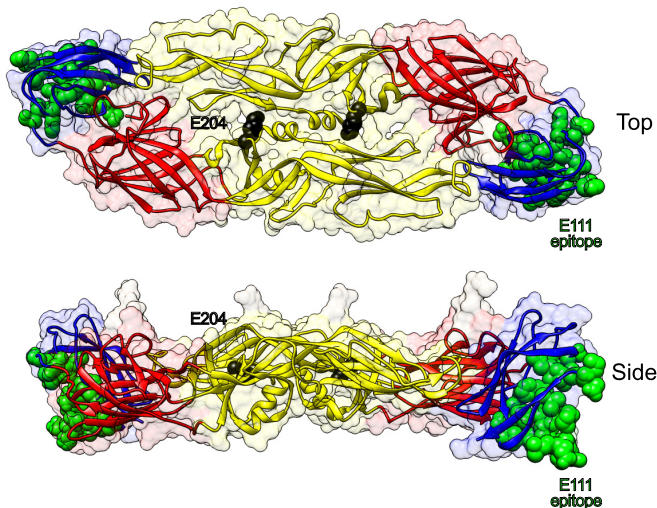

FIG 4 E residue 204 is located at a distance from the E111 epitope. The structure of the DENV E protein dimer (PDB accession no. 1OAN) is shown in ribbon form from the top and side view relative to the arrangement on the mature virion. Domains I, II, and III are colored in red, yellow, and blue, respectively. E residue 204, located within domain II, is highlighted in black, while the residues that comprise the domain III epitope of E111 are shown in green. On the E monomer, residue 204 is located ~54 Å from the crystallographically defined E111 epitope.

not fully recapitulate the EC_{50}s observed against the wild-type strains ($P \leq 0.012$ for comparisons of 204/345 variants to nonparental wild-type strain EC_{50}s) (Fig. 5A and E). While we were unable to identify the amino acid(s) responsible for the relatively modest (<5-fold) difference in E111 neutralization potency that remained among comparisons of wild-type 16007 versus WP-74 K204R and wild-type WP-74 versus 16007 R204K RVPs, the presence of a lysine versus arginine at E-204 clearly represents the primary cause of the observed 175-fold difference in neutralization sensitivity between strains WP-74 and 16007.

Variation at E protein residue 204 impacts the stability of infectious DENV1 in solution. We have hypothesized that the dynamics of flavivirus E proteins that characterize virus breathing result in both reversible and nonreversible changes in virus structure (15). Nonreversible changes have the potential to generate virus structures no longer capable of mediating infectivity; these would be detected experimentally as a loss of infectivity over time (referred to as intrinsic decay). The rate at which flaviviruses lose infectivity, or decay, in solution varies (29), even within populations of genetically identical viruses that differ only by the extent of virus maturation (15). One explanation of this variability is that differences in the ensemble of structures sampled by each virus impact the rate at which noninfectious conformations accumulate among distinct virus populations.

We hypothesized that differences in the structural dynamics of virus strains 16007 and WP-74 regulated by residue E-204 would accompany changes in intrinsic decay. To investigate this, we first incubated wild-type 16007 and WP-74 RVPs at 37°C, harvesting
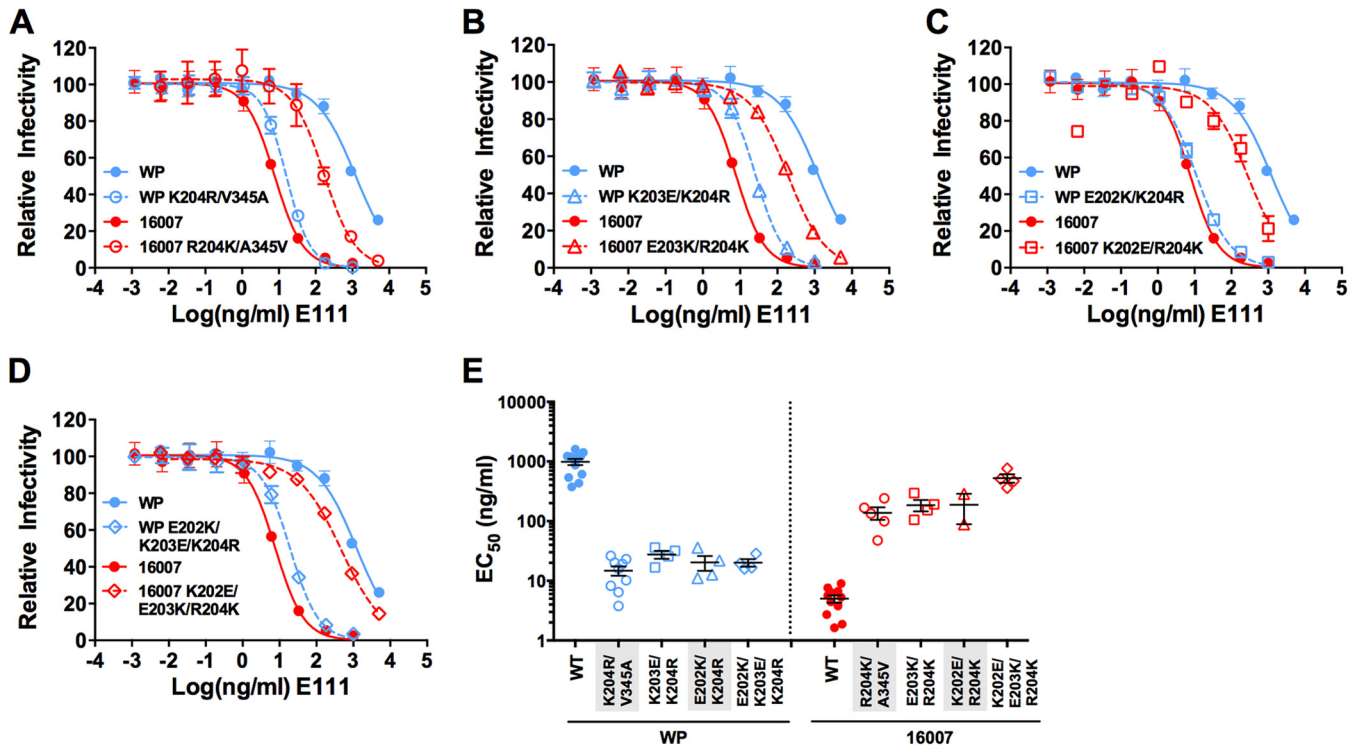
FIG 5 Effects of E residue 204 on E111 neutralization of 16007 and WP-74 RVPs. Dose-response neutralization profiles were generated by incubating RVPs with serial dilutions of the MAb E111 for 1 h at 37°C, followed by addition of Raji-DCSIGNR cells. After 48 h, the number of infected, GFP-positive cells was determined by flow cytometry. The resulting data were fit by nonlinear regression (variable slope) to predict the EC_{50}. (A to D) Representative E111 neutralization profiles against wild-type (WT) 16007 and WP-74 (WP) RVPs compared to mutant RVPs expressing combinations of reciprocal amino acid substitutions at E residues 204 and 345, 202 and 204, 203 and 204, and 202, 203, and 204, respectively. Error bars represent the range of duplicate infections. (E) EC_{50}s from 2 to 12 independent experiments per RVP. The horizontal line and error bars represent the mean and range or standard error, respectively.

samples at incremental times for the next 72 h. The infectivity of the individual samples was determined by infecting Raji cells expressing the attachment factor DC-SIGNR (Raji-DCSIGNR), and the resulting data fit to a one-phase decay curve to estimate the half-life of RVP infectivity (Fig. 6A and D). We observed that the loss of WP-74 infectivity occurred 1.95 times faster than that for 16007 ($P = 0.01$, comparison of mean infectivity half-life values for 16007 versus WP-74). Repeating this assay with WP-74 K204R and 16007 R204K variants revealed that this ~2-fold difference in the half-life of 16007 and WP-74 infectivity in solution also tracked with residue E-204 (Fig. 6B, C, and D). The mean half-lives of infectivity for WP-74 versus 16007 R204K were 3.2 and 2.0 h, respectively ($P = 0.093$), and for 16007 versus WP-74 K204R, the values were 6.2 and 5.6, respectively ($P = 0.389$). When the half-life of infectivity was measured for a selection of other variants, none differed from the parental wild-type strain (data not shown). That a residue located in E-DII can impact accessibility of the otherwise cryptic E-DIII E111 epitope as well as the rate of intrinsic decay for strains WP-74 and 16007 suggests a structural basis for these differences.

Variation at E protein residue 204 broadly impacts neutralization potency of antibodies targeting DIII. We next assessed neutralization of wild-type and residue 204 variant RVPs with four additional MAbs of varying specificities (Fig. 7). MAbs E98, E102, and E106 are DENV1 type-specific MAbs that bind epitopes in E-DIII that are distinct from that of MAb E111 (28). Similar to MAb E111, these three MAbs displayed greater neutralization po-

tency against strain 16007 than against strain WP-74, and these differences in susceptibility tracked completely with the amino acid at residue 204 (Fig. 7B to E). In contrast, the E-DII fusion loop-specific MAb E60 neutralized all variants equivalently (Fig. 7A and E). Taken together, these results indicate that variation at E-DII residue 204 results in regional antibody accessibility differences among strains WP-74 and 16007.

DISCUSSION

Development of a DENV vaccine is complicated by the need to induce protective antibodies against all four DENV serotypes. *In vitro* assays that predict protection from DENV infection have not been validated. While experience with existing human flavivirus vaccines suggests that neutralizing antibody titers correlate with protection from DENV disease (30–33), recent phase III clinical trials of the CYD tetravalent DENV vaccine candidate performed in Latin America and Asia do not support this assertion. Despite the presence of neutralizing antibodies against all four serotypes, overall protective efficacy was only ~60% and varied considerably (35% to 78%) among DENV serotypes (34, 35). Relationships between vaccine-induced neutralizing antibodies and protection from infection remain incompletely understood and cannot be inferred from the mean neutralization titers reported in clinical studies. Furthermore, whether the type and interpretation of existing neutralization assays correlate with protective and nonprotective antibody responses requires further study (36).

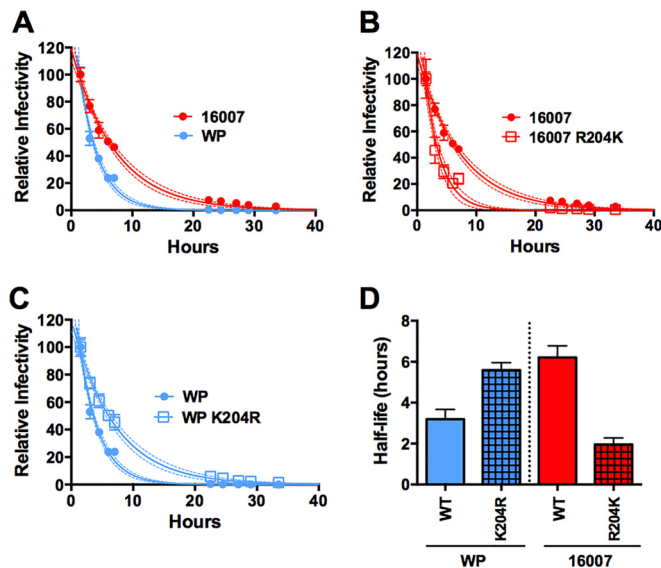How sequence differences among distinct DENV serotypes

FIG 6 Intrinsic decay of DENV1 strains 16007 and WP-74 infectivity. Populations of 16007 and WP-74 RVPs were equilibrated to 37°C, after which samples were harvested and frozen at the indicated times. The infectivity at each point was determined by infection of Raji-DCSIGNR cells and monitored by flow cytometry 48 h postinfection. The data are normalized to the infectivity of RVPs at the initial time point (after the 1-h 37°C preincubation) and fitted to a single-phase exponential decay curve to obtain the half-life. (A to C) Representative experiments comparing wild-type (WT) 16007 versus WP-74 (WP) (A), wild-type 16007 versus 16007 R204K (B), and wild-type WP-74 versus WP-74 K204R (C). The 95% confidence intervals are indicated by the dotted lines, and error bars represent the standard error of triplicate measurements. (D) The results of four (wild-type 16007 and 16007 R204K) or five (wild-type WP-74 and WP-74 K204R) individual experiments per RVP, each performed in triplicate, are shown. Error bars represent the standard error, and the horizontal line shows the mean of all experiments.

and strains impact the protective efficacy of neutralizing antibodies is not understood. Several recent studies of DENV MAbs suggest that genotypic differences in neutralization exist (28, 37–41). In this study, we investigated the molecular basis for significant differences in the neutralization sensitivity among two closely related DENV1 strains representing distinct genotypes. The DENV1 type-specific MAb E111 inhibits infection of the DENV1 strain 16007 at antibody concentrations markedly lower than the amount required to neutralize the WP-74 strain (23, 28). We identified a single amino acid residue on the E protein (residue 204) capable of altering neutralization potency at a site distant from the crystallographically defined E111 epitope-paratope interface (Fig. 4) (23). The conservative lysine-to-arginine substitution impacted sensitivity to numerous DIII-reactive MAbs as well as the stability of the RVPs in solution. These patterns of neutralization sensitivity were further confirmed by neutralization assays performed using Vero cells that do not express the attachment factor DC-SIGNR and with K562 cells that express the Fc receptor CD32 (data not shown). Our data suggest that position 204 regulates epitope accessibility on E-DIII through changes in the ensemble of structures sampled through viral breathing. Our results provide a striking example in which minor sequence variation among DENV strains can result in unexpectedly broad consequences impacting both the biology of the virus and the antiviral immune response.

Viral breathing alters epitope accessibility and recognition. Cryo-electron microscopy (Cryo-EM) reconstruction of the mature flavivirus virion revealed a smooth particle containing 90 head-to-tail E protein dimers (6, 42). Unexpectedly, numerous examples of neutralizing MAbs that map to regions not predicted to be accessible on this structure have been reported (9, 23–25, 27). Antibody recognition of cryptic epitopes can be explained in part by the finding that flavivirus maturation is not efficient, resulting in the presence of uncleaved prM on infectious virions (43). These partially mature virus particles retain structural characteristics of both mature and immature forms of the virus (44). This structural heterogeneity governs the array of epitopes accessible for antibody binding, and thus, the neutralization potency of many flavivirus-specific antibodies (45). However, the structural basis for recognition by many antibodies remains unexplained, as the epitopes for these antibodies map to regions not predicted to be accessible on models of the immature or mature forms of the virus.

The phenomenon of viral breathing has been extensively studied with nonenveloped picornaviruses. Early antigenic mapping studies of poliovirus identified neutralizing antisera that bound N-terminal peptides of the capsid protein VP1 (46, 47). However, the X-ray crystal structure of the virus subsequently revealed that this region of VP1 is situated on the interior of the virion, suggesting that multiple conformations of poliovirus capsid exist (48). Antibodies specific for internal portions of the capsids of several picornaviruses (including the N termini of VP1 and VP4) exhibit time- and temperature-dependent patterns of neutralization (12, 49, 50). While not understood in structural detail, the surface glycoproteins of enveloped viruses also breathe. The neutralizing MAb Y8-10C2 binds an epitope on the influenza virus hemagglutinin trimer that is exposed only with increased incubation time or temperature (13). More recently, an elegant study of HIV-1 used single-molecule fluorescence energy transfer to identify three unliganded states of the HIV-1 envelope trimer (51). Thus, an ensemble of gp120 structures may impact the mechanics of virus entry and sensitivity to antibody neutralization.

Antibodies have also served as useful probes for flavivirus dynamics. Structural studies of DENV2 in complex with Fab fragments of the neutralizing MAb 1A1D-2 revealed that substantial E protein rearrangements were required to accommodate antibody binding to an otherwise inaccessible epitope on the A-strand of E-DIII. Furthermore, these transitions required incubation at physiological temperature, as binding occurred at 37°C, but not at 4°C (24). The results of these studies suggested that temperature-dependent changes in structure regulated epitope accessibility. Structural studies of DENV recognition by MAb 4E11, another E-DIII A-strand-reactive antibody, reached a similar conclusion (52, 53). We have shown that the binding of antibody to many poorly accessible West Nile virus (WNV) and DENV epitopes display time- and temperature-dependent patterns of neutralization (14, 15). Similar findings were reported with the hepatitis C virus (16). Importantly, antibody order-of-addition studies performed with WNV and DENV demonstrated that changes in viral structure associated with increases in neutralization sensitivity were reversible (15), analogous to prior studies of viral breathing with picornaviruses (12).

Intrinsic decay of flavivirus infectivity. Prolonged incubation of viruses in solution results in a loss of infectivity. We have shown previously that the stability of WNV and DENV varies (15, 29).
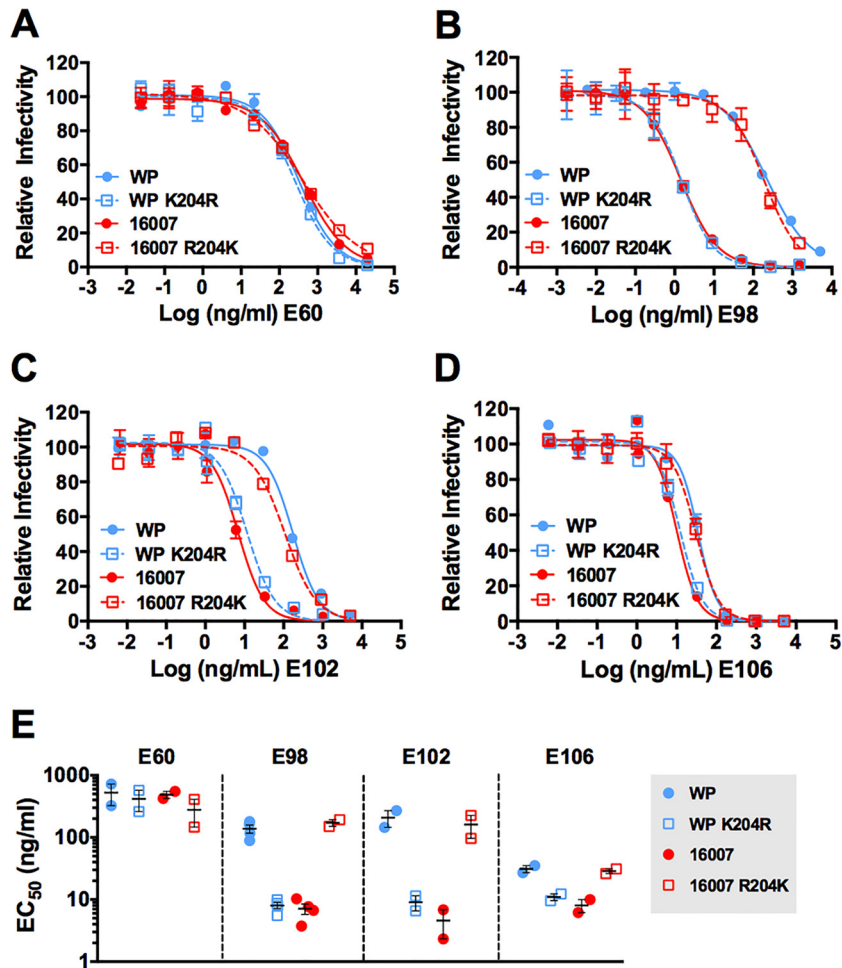
FIG 7 E residue 204 broadly impacts neutralization sensitivity to MAbs targeting DIII epitopes. Dose-response neutralization profiles were generated by incubating RVPs with serial dilutions of the indicated MAbs for 1 h at 37°C, followed by addition of Raji-DCSIGNR cells. After 48 h, the number of infected, GFP-positive cells was determined by flow cytometry. The resulting data were fit by nonlinear regression (variable slope) to predict the EC_{50}. (A to D) Representative neutralization profiles for 16007, WP-74 (WP), 16007 R204K, and WP-74 K204R RVPs with the MAbs E60 (WNV specific; cross-reactive for DENV E-DII fusion loop) (A), E98 (E-DIII A-strand) (B), E102 (E-DIII BC loop) (C), and E106 (E-DIII A-strand) (D). Error bars represent the range of duplicate infections. (E) EC_{50}s from two to four independent experiments per RVP-MAb pair. The horizontal line and error bars represent the mean and range or standard error, respectively.

Our hypothesis is that the time- and temperature-dependent reduction in the infectivity of flaviviruses in solution reflects the sampling of E protein conformations from which it is energetically unfavorable to return to an infectious state. Herein, we demonstrate that a conservative mutation that modulates accessibility of the E111 epitope also controls the stability of the virion in solution. Altering position 204 of DENV1 WP-74 from a lysine to an arginine resulted in RVPs that were more sensitive to neutralization by MAb E111 and had a lower rate of decay as measured by the loss of infectivity in solution in the absence of antibody. The converse was true when DENV1 16007 residue 204 was changed from an arginine to a lysine. Because we have limited structural insights into the ensemble of structures that exist at physiological temperatures (beyond the observation that they are very heterogeneous), understanding the precise mechanisms that underlie this relationship is not currently possible.

The intrinsic decay of flavivirus infection may be analogous to the formation of the altered particle (A-particle) of some picorna-viruses (54, 55). The A-particle is thought to be an intermediate structure that occurs during cell entry and viral uncoating. However, the transition to this structure can occur in solution at equilibrium (56, 57), and the rate of this change can be enhanced by the presence of a receptor or increased temperature (58, 59). These findings suggest that the A-particle structure is included in the conformational ensemble sampled during virus breathing, albeit infrequently in the absence of receptor. Future studies performed with an array of flavivirus strains and antibodies with different specificities may help clarify the relationship between virus breathing, antibody accessibility, and intrinsic decay.

Implications of viral breathing. How does sequence diversity among DENV strains impact dynamics? Genotypic differences in MAb neutralization have been observed for all four DENV serotypes (28, 37, 39, 40), despite limited sequence diversity (≤3%) at the amino acid level. Our results indicate that a single amino acid difference can impact neutralization potency not only through direct antibody-paratope interactions but also via changes in the

structural dynamics of the virion. The location of the E-204 residue in the E protein dimer may ultimately provide insight into understanding strain-specific differences in virus breathing. The interactions among E proteins that contribute to virus stability have not been experimentally tested, and they may include contacts at the dimer interface, between dimers, or among rafts (11). For example, comparisons of the crystal structures of various flavivirus E proteins identify differences in the surface area of these dimer interface contacts; whether recombinant forms of flavivirus E proteins are found as a monomer or dimer in solution is likely related to the size and strength of these contacts (60). Interestingly, E protein residue 204 is located at this dimer interface of adjacent E proteins (Fig. 4). The presence of a lysine (WP-74) versus arginine (16007) may influence the strength of this interaction, which in turn shapes the structural ensembles sampled by each strain. Curiously, a 16007 variant with a much less chemically conservative side chain (16007 R204D) behaved identically to wild-type 16007 in E111 neutralization experiments (L. A. Vanblargan, K. A. Dowd, and T. C. Pierson, unpublished data), highlighting difficulties in drawing conclusions based on the chemical properties of different amino acid side chains at this location. Ultimately, the identification of additional mutations that alter epitope accessibility and virus particle stability will be required to identify features of the mature virion with the potential to stabilize the virion or impart conformational flexibility. Our observation that E protein residue 204 altered access to a cryptic DIII epitope, but not a well-characterized DII epitope, suggests that local control is possible. Efforts are under way to introduce mutations at E protein position 204 of an infectious molecular clone of DENV1 WP-74. This construct will allow study of the impact of viral breathing on virus replication, pathogenesis, and immunogenicity. Preliminary studies indicate that E residue 204 is a site for the introduction of mutations associated with adaptation to cell culture, highlighting both the technical challenges and importance of understanding the biology of variation at this and other positions that impact the conformational dynamics of the virion.

In summary, we identified a single amino acid difference within E-DII of DENV1 strains WP-74 and 16007 that impacts neutralization potency of a group of E-DIII-specific MAbs at a distance. Changes at this position also modulate the intrinsic decay rate of RVP infectivity, suggesting that residue 204 is involved in contacts that hold together the lattice of E proteins that comprise the surface of the mature virus. Our studies indicate a role for sequence variation in modulating virus structure and stability. These results are of particular importance to the design and interpretation of ongoing DENV vaccine efforts.

MATERIALS AND METHODS

Cell lines. Cell lines were maintained at 37°C in the presence of 7% CO_2. HEK-293T cells were grown in complete Dulbecco's modified Eagle medium (DMEM) containing GlutaMAX and supplemented with 7% fetal bovine serum (FBS) and 100 U/ml penicillin-streptomycin (PS). When producing virus particles, a low-glucose formulation of DMEM containing HEPES, also supplemented with 7% FBS and 100 U/ml PS, was substituted. Use of this medium slows the rate of medium acidification, which has the potential to prematurely trigger (and thus inactivate) flaviviruses. Raji cells expressing the attachment factor DC-SIGNR (Raji-DCSIGNR) were maintained in RPMI 1640 medium containing GlutaMAX and supplemented with 7% FBS and 100 U/ml PS. All tissue culture media and supplements were supplied by Life Technologies (Carlsbad, CA).

Production of DENV RVPs. Reporter virus particles (RVPs) were generated by cotransfection of a viral subgenomic replicon with the structural genes in *trans*, resulting in virions capable of only a single round of infection. A green fluorescent protein (GFP) reporter gene in the replicon allows for productive infection of target cells to be quantitated by flow cytometry (29, 61). In the current study, DENV RVPs were generated by cotransfection of HEK-293T cells with a plasmid encoding the structural genes (C-prM-E) of DENV serotype 1 (DENV1) and a WNV lineage II replicon that expresses GFP (using a 3:1 ratio of plasmid DNA by mass, respectively). Transfected cells were incubated at 30°C. RVP-containing supernatants were harvested between 72 and 120 h posttransfection, filtered through a 0.2-μm membrane, and frozen as aliquots at −80°C. Titer data were obtained by infecting Raji-DCSIGNR cells with serial twofold dilutions of RVPs at 37°C. Infection was assessed by GFP expression 48 h postinfection using flow cytometry.

DENV structural gene constructs used for RVP production. DENV RVPs were generated with plasmids expressing wild-type and mutant variants of the structural genes from serotype 1 strains Western Pacific-74 (WP-74) and 16007. Cloning of variants was done by using two methods. (i) E protein chimeras between WP-74 and 16007 were generated using overlap-extension PCR. The resulting C-prM-E PCR fragments were cloned into a mammalian expression vector using either Gateway (Life Technologies, Carlsbad, CA) or In-Fusion (Clontech, Mountain View, CA) technologies, per the manufacturer's instructions. In all chimera constructs, the C-prM sequence is provided by the strain that comprises the 5′ end of the E protein chimera. (ii) Mutants containing one, two, or three reciprocal amino acid differences between strains WP-74 and 16007 were generated using the QuikChange site-directed mutagenesis kit (Stratagene, La Jolla, CA). Variants were fully sequenced before use in cotransfection experiments to generate RVPs.

Neutralization dose-response studies. Determining the neutralization potency of monoclonal antibodies (MAbs) against RVPs has been previously described (14, 45, 62). RVPs were sufficiently diluted to ensure antibody excess at informative points of the dose-response curve and incubated with nine serial dilutions of the indicated MAbs for 1 h at 37°C to allow for steady-state binding (14). Following this preincubation, antibody-RVP complexes were used to infect Raji-DCSIGNR cells in duplicate. Infections were carried out at 37°C, and infectivity was monitored by flow cytometry 48 h later. Neutralization results were analyzed by nonlinear regression (using a variable slope) to estimate the 50% effective concentration (EC_{50}) value (Prism; GraphPad Software, La Jolla, CA).

RVP intrinsic decay curves. RVP stocks were diluted to the same level of infection used in neutralization studies. After diluted RVP stocks were equilibrated to 37°C for approximately 1 h, samples were further incubated at 37°C for up to 72 h. At the indicated times, aliquots were removed and frozen at −80°C. All frozen samples from a given experiment were thawed simultaneously and used to infect Raji-DCSIGNR cells in triplicate. Infectivity was determined 48 h postinfection by flow cytometry and normalized to levels obtained immediately after the preincubation step. Results were fitted with a single-phase exponential decay curve to estimate the half-life of infectivity (Prism; GraphPad Software, La Jolla, CA).

Statistical analysis. Statistical analyses were performed using Prism software (GraphPad Software, La Jolla, CA). EC_{50}s were log transformed, and the data in Fig. 1, 3, and 5 were analyzed via one-way analysis of variance (ANOVA) (wild-type WP-74 versus WP-74 mutants and wild-type 16007 versus 16007 mutants separately for Fig. 1 and 3; wild-type WP-74 versus 16007 mutants and wild-type 16007 versus WP-74 mutants separately in Fig. 5) followed by Dunnett's correction for multiple comparisons. *P* values with this correction are reported throughout the manuscript. Infectivity half-life values were log transformed, and two-way comparisons were performed using a two-tailed, unpaired Student's *t* test.

REFERENCES

1. **Bhatt S, Gething PW, Brady OJ, Messina JP, Farlow AW, Moyes CL, Drake JM, Brownstein JS, Hoen AG, Sankoh O, Myers MF, George DB, Jaenisch T, Wint GRW, Simmons CP, Scott TW, Farrar JJ, Hay SI.** 2013. The global distribution and burden of dengue. Nature **496:**504–507. http://dx.doi.org/10.1038/nature12060.

2. **Kaufmann B, Rossmann MG.** 2011. Molecular mechanisms involved in the early steps of flavivirus cell entry. Microbes Infect **13:**1–9. http://dx.doi.org/10.1016/j.micinf.2010.09.005.

3. **Holmes EC, Twiddy SS.** 2003. The origin, emergence and evolutionary genetics of dengue virus. Infect Genet Evol **3:**19–28. http://dx.doi.org/10.1016/S1567-1348(03)00004-2.

4. **Rico-Hesse R.** 1990. Molecular evolution and distribution of dengue viruses type 1 and 2 in nature. Virology **174:**479–493. http://dx.doi.org/10.1016/0042-6822(90)90102-W.

5. **Goncalvez AP, Escalante AA, Pujol FH, Ludert JE, Tovar D, Salas RA, Liprandi F.** 2002. Diversity and evolution of the envelope gene of dengue virus type 1. Virology **303:**110–119. http://dx.doi.org/10.1006/viro.2002.1686.

6. **Kuhn RJ, Zhang W, Rossmann MG, Pletnev SV, Corver J, Lenches E, Jones CT, Mukhopadhyay S, Chipman PR, Strauss EG, Baker TS, Strauss JH.** 2002. Structure of dengue virus: implications for flavivirus organization, maturation, and fusion. Cell **108:**717–725. http://dx.doi.org/10.1016/S0092-8674(02)00660-8.

7. **Zhang X, Ge P, Yu X, Brannan JM, Bi G, Zhang Q, Schein S, Zhou ZH.** 2013. Cryo-EM structure of the mature dengue virus at 3.5-A resolution. Nat Struct Mol Biol **20:**105–110. http://dx.doi.org/10.1038/nsmb.2463.

8. **Pierson TC, Fremont DH, Kuhn RJ, Diamond MS.** 2008. Structural insights into the mechanisms of antibody-mediated neutralization of flavivirus infection: implications for vaccine development. Cell Host Microbe **4:**229–238. http://dx.doi.org/10.1016/j.chom.2008.08.004.

9. **Stiasny K, Kiermayr S, Holzmann H, Heinz FX.** 2006. Cryptic properties of a cluster of dominant flavivirus cross-reactive antigenic sites. J Virol **80:**9557–9568. http://dx.doi.org/10.1128/JVI.00080-06.

10. **Crill WD, Roehrig JT.** 2001. Monoclonal antibodies that bind to domain III of dengue virus E glycoprotein are the most efficient blockers of virus adsorption to Vero cells. J Virol **75:**7769–7773. http://dx.doi.org/10.1128/JVI.75.16.7769-7773.2001.

11. **Kuhn RJ, Dowd KA, Beth Post C, Pierson TC.** 2015. Shake, rattle, and roll: impact of the dynamics of flavivirus particles on their interactions with the host. Virology **479-480:**508–517. http://dx.doi.org/10.1016/j.virol.2015.03.025.

12. **Li Q, Yafal AG, Lee YM, Hogle J, Chow M.** 1994. Poliovirus neutralization by antibodies to internal epitopes of VP4 and VP1 results from reversible exposure of these sequences at physiological temperature. J Virol **68:**3965–3970.

13. **Yewdell JW, Taylor A, Yellen A, Caton A, Gerhard W, Bachi T.** 1993. Mutations in or near the fusion peptide of the influenza virus hemagglutinin affect an antigenic site in the globular region. J Virol **67:**933–942.

14. **Dowd KA, Jost CA, Durbin AP, Whitehead SS, Pierson TC.** 2011. A dynamic landscape for antibody binding modulates antibody-mediated neutralization of West Nile virus. PLoS Pathog **7:**e1002111. http://dx.doi.org/10.1371/journal.ppat.1002111.

15. **Dowd KA, Mukherjee S, Kuhn RJ, Pierson TC.** 2014. Combined effects of the structural heterogeneity and dynamics of flaviviruses on antibody recognition. J Virol **88:**11726–11737. http://dx.doi.org/10.1128/JVI.01140-14.

16. **Sabo MC, Luca VC, Ray SC, Bukh J, Fremont DH, Diamond MS.** 2012. Hepatitis C virus epitope exposure and neutralization by antibodies is affected by time and temperature. Virology **422:**174–184. http://dx.doi.org/10.1016/j.virol.2011.10.023.

17. **Lewis JK, Bothner B, Smith TJ, Siuzdak G.** 1998. Antiviral agent blocks breathing of the common cold virus. Proc Natl Acad Sci U S A **95:**6774–6778. http://dx.doi.org/10.1073/pnas.95.12.6774.

18. **Roy A, Post CB.** 2012. Long-distance correlations of rhinovirus capsid dynamics contribute to uncoating and antiviral activity. Proc Natl Acad Sci U S A **109:**5271–5276. http://dx.doi.org/10.1073/pnas.1119174109.

19. **Fibriansah G, Ng TS, Kostyuchenko VA, Lee J, Lee S, Wang J, Lok SM.** 2013. Structural changes in dengue virus when exposed to a temperature of 37°C. J Virol **87:**7585–7592. http://dx.doi.org/10.1128/JVI.00757-13.

20. **Zhang X, Sheng J, Plevka P, Kuhn RJ, Diamond MS, Rossmann MG.** 2013. Dengue structure differs at the temperatures of its human and mosquito hosts. Proc Natl Acad Sci U S A **110:**6795–6799. http://dx.doi.org/10.1073/pnas.1304300110.

21. **Kostyuchenko VA, Chew PL, Ng TS, Lok SM.** 2014. Near-atomic resolution cryo-electron microscopic structure of dengue serotype 4 virus. J Virol **88:**477–482. http://dx.doi.org/10.1128/JVI.02641-13.

22. **Whitehead SS, Blaney JE, Durbin AP, Murphy BR.** 2007. Prospects for a dengue virus vaccine. Nat Rev Microbiol **5:**518–528. http://dx.doi.org/10.1038/nrmicro1690.

23. **Austin SK, Dowd KA, Shrestha B, Nelson CA, Edeling MA, Johnson S, Pierson TC, Diamond MS, Fremont DH.** 2012. Structural basis of differential neutralization of DENV-1 genotypes by an antibody that recognizes a cryptic epitope. PLoS Pathog **8:**e1002930. http://dx.doi.org/10.1371/journal.ppat.1002930.

24. **Lok SM, Kostyuchenko V, Nybakken GE, Holdaway HA, Battisti AJ, Sukupolvi-Petty S, Sedlak D, Fremont DH, Chipman PR, Roehrig JT, Diamond MS, Kuhn RJ, Rossmann MG.** 2008. Binding of a neutralizing antibody to dengue virus alters the arrangement of surface glycoproteins. Nat Struct Mol Biol **15:**312–317. http://dx.doi.org/10.1038/nsmb.1382.

25. **Nybakken GE, Oliphant T, Johnson S, Burke S, Diamond MS, Fremont DH.** 2005. Structural basis of West Nile virus neutralization by a therapeutic antibody. Nature **437:**764–769. http://dx.doi.org/10.1038/nature03956.

26. **Oliphant T, Engle M, Nybakken GE, Doane C, Johnson S, Huang L, Gorlatov S, Mehlhop E, Marri A, Chung KM, Ebel GD, Kramer LD, Fremont DH, Diamond MS.** 2005. Development of a humanized monoclonal antibody with therapeutic potential against West Nile virus. Nat Med **11:**522–530. http://dx.doi.org/10.1038/nm1240.

27. **Oliphant T, Nybakken GE, Engle M, Xu Q, Nelson CA, Sukupolvi-Petty S, Marri A, Lachmi BE, Olshevsky U, Fremont DH, Pierson TC, Diamond MS.** 2006. Antibody recognition and neutralization determinants on domains I and II of West Nile virus envelope protein. J Virol **80:**12149–12159. http://dx.doi.org/10.1128/JVI.01732-06.

28. **Shrestha B, Brien JD, Sukupolvi-Petty S, Austin SK, Edeling MA, Kim T, O'Brien KM, Nelson CA, Johnson S, Fremont DH, Diamond MS.** 2010. The development of therapeutic antibodies that target homologous and heterologous genotypes of dengue virus type 1. PLoS Pathog **6:**e1000823. http://dx.doi.org/10.1371/journal.ppat.1000823.

29. **Ansarah-Sobrinho C, Nelson S, Jost CA, Whitehead SS, Pierson TC.** 2008. Temperature-dependent production of pseudoinfectious dengue reporter virus particles by complementation. Virology **381:**67–74. http://dx.doi.org/10.1016/j.virol.2008.08.021.

30. **Belmusto-Worn VE, Sanchez JL, McCarthy K, Nichols R, Bautista CT, Magill AJ, Pastor-Cauna G, Echevarria C, Laguna-Torres VA, Samame BK, Baldeon ME, Burans JP, Olson JG, Bedford P, Kitchener S, Monath TP.** 2005. Randomized, double-blind, phase III, pivotal field trial of the comparative immunogenicity, safety, and tolerability of two yellow fever 17D vaccines (Arilvax and YF-VAX) in healthy infants and children in Peru. Am J Trop Med Hyg **72:**189–197.

31. **Heinz FX, Holzmann H, Essl A, Kundi M.** 2007. Field effectiveness of vaccination against tick-borne encephalitis. Vaccine **25:**7559–7567. http://dx.doi.org/10.1016/j.vaccine.2007.08.024.

32. **Mason RA, Tauraso NM, Spertzel RO, Ginn RK.** 1973. Yellow fever vaccine: direct challenge of monkeys given graded doses of 17D vaccine. Appl Microbiol **25:**539–544.

33. **Monath TP, Nichols R, Archambault WT, Moore L, Marchesani R, Tian J, Shope RE, Thomas N, Schrader R, Furby D, Bedford P.** 2002. Comparative safety and immunogenicity of two yellow fever 17D vaccines (ARILVAX and YF-VAX) in a phase III multicenter, double-blind clinical trial. Am J Trop Med Hyg **66:**533–541.

34. **Capeding MR, Tran NH, Hadinegoro SR, Ismail HI, Chotpitayasunondh T, Chua MN, Luong CQ, Rusmil K, Wirawan DN, Nallusamy R, Pitisuttithum P, Thisyakorn U, Yoon IK, van der Vliet D, Langevin E, Laot T, Hutagalung Y, Frago C, Boaz M, Wartel TA, Tornieporth NG, Saville M, Bouckenooghe A, CYD14 Study Group.** 2014. Clinical efficacy and safety of a novel tetravalent dengue vaccine in healthy children in Asia: a phase 3, randomised, observer-masked, placebo-controlled trial. Lancet **384:**1358–1365. http://dx.doi.org/10.1016/S0140-6736(14)61060-6.

35. **Villar L, Dayan GH, Arredondo-Garcia JL, Rivera DM, Cunha R,**

Deseda C, Reynales H, Costa MS, Morales-Ramirez JO, Carrasquilla G, Rey LC, Dietze R, Luz K, Rivas E, Miranda Montoya MC, Cortes Supelano M, Zambrano B, Langevin E, Boaz M, Tornieporth N, Saville M, Noriega F, CYD14 Study Group. 2015. Efficacy of a tetravalent dengue vaccine in children in Latin America. N Engl J Med 372:113–123. http://dx.doi.org/10.1056/NEJMoa1411037.

36. Diamond MS, Pierson TC, Fremont DH. 2008. The structural immunology of antibody protection against West Nile virus. Immunol Rev 225:212–225. http://dx.doi.org/10.1111/j.1600-065X.2008.00676.x.

37. Brien JD, Austin SK, Sukupolvi-Petty S, O'Brien KM, Johnson S, Fremont DH, Diamond MS. 2010. Genotype-specific neutralization and protection by antibodies against dengue virus type 3. J Virol 84:10630–10643. http://dx.doi.org/10.1128/JVI.01190-10.

38. Lanciotti RS, Gubler DJ, Trent DW. 1997. Molecular evolution and phylogeny of dengue-4 viruses. J Gen Virol 78:2279–2284. http://dx.doi.org/10.1099/0022-1317-78-9-2279.

39. Sukupolvi-Petty S, Austin SK, Engle M, Brien JD, Dowd KA, Williams KL, Johnson S, Rico-Hesse R, Harris E, Pierson TC, Fremont DH, Diamond MS. 2010. Structure and function analysis of therapeutic monoclonal antibodies against dengue virus type 2. J Virol 84:9227–9239. http://dx.doi.org/10.1128/JVI.01087-10.

40. Sukupolvi-Petty S, Brien JD, Austin SK, Shrestha B, Swayne S, Kahle K, Doranz BJ, Johnson S, Pierson TC, Fremont DH, Diamond MS. 2013. Functional analysis of antibodies against dengue virus type 4 reveals strain-dependent epitope exposure that impacts neutralization and protection. J Virol 87:8826–8842. http://dx.doi.org/10.1128/JVI.01314-13.

41. Wahala WMPB, Donaldson EF, de Alwis R, Accavitti-Loper MA, Baric RS, de Silva AM. 2010. Natural strain variation and antibody neutralization of dengue serotype 3 viruses. PLoS Pathog 6:e1000821. http://dx.doi.org/10.1371/journal.ppat.1000821.

42. Mukhopadhyay S, Kim BS, Chipman PR, Rossmann MG, Kuhn RJ. 2003. Structure of West Nile virus. Science 302:248. http://dx.doi.org/10.1126/science.1089316.

43. Pierson TC, Diamond MS. 2012. Degrees of maturity: the complex structure and biology of flaviviruses. Curr Opin Virol 2:168–175. http://dx.doi.org/10.1016/j.coviro.2012.02.011.

44. Plevka P, Battisti AJ, Junjhon J, Winkler DC, Holdaway HA, Keelapang P, Sittisombut N, Kuhn RJ, Steven AC, Rossmann MG. 2011. Maturation of flaviviruses starts from one or more icosahedrally independent nucleation centres. EMBO Rep 12:602–606. http://dx.doi.org/10.1038/embor.2011.75.

45. Nelson S, Jost CA, Xu Q, Ess J, Martin JE, Oliphant T, Whitehead SS, Durbin AP, Graham BS, Diamond MS, Pierson TC. 2008. Maturation of West Nile virus modulates sensitivity to antibody-mediated neutralization. PLoS Pathog 4:e1000060. http://dx.doi.org/10.1371/journal.ppat.1000060.

46. Chow M, Yabrov R, Bittle J, Hogle J, Baltimore D. 1985. Synthetic peptides from four separate regions of the poliovirus type 1 capsid protein VP1 induce neutralizing antibodies. Proc Natl Acad Sci U S A 82:910–914. http://dx.doi.org/10.1073/pnas.82.3.910.

47. Emini EA, Jameson BA, Wimmer E. 1983. Priming for and induction of anti-poliovirus neutralizing antibodies by synthetic peptides. Nature 304:699–703. http://dx.doi.org/10.1038/304699a0.

48. Hogle JM, Chow M, Filman DJ. 1985. Three-dimensional structure of poliovirus at 2.9-A resolution. Science 229:1358–1365. http://dx.doi.org/10.1126/science.2994218.

49. Katpally U, Fu TM, Freed DC, Casimiro DR, Smith TJ. 2009. Antibodies to the buried N terminus of rhinovirus VP4 exhibit cross-serotypic neutralization. J Virol 83:7040–7048. http://dx.doi.org/10.1128/JVI.00557-09.

50. Pulli T, Lankinen H, Roivainen M, Hyypiä T. 1998. Antigenic sites of coxsackievirus A9. Virology 240:202–212. http://dx.doi.org/10.1006/viro.1997.8908.

51. Munro JB, Gorman J, Ma X, Zhou Z, Arthos J, Burton DR, Koff WC, Courter JR, Smith AB, III, Kwong PD, Blanchard SC, Mothes W. 2014. Conformational dynamics of single HIV-1 envelope trimers on the surface of native virions. Science 346:759–763. http://dx.doi.org/10.1126/science.1254426.

52. Cockburn JJ, Navarro Sanchez ME, Goncalvez AP, Zaitseva E, Stura EA, Kikuti CM, Duquerroy S, Dussart P, Chernomordik LV, Lai CJ, Rey FA. 2012. Structural insights into the neutralization mechanism of a higher primate antibody against dengue virus. EMBO J 31:767–779. http://dx.doi.org/10.1038/emboj.2011.439.

53. Pierson TC, Kuhn RJ. 2012. Capturing a virus while it catches its breath. Structure 20:200–202. http://dx.doi.org/10.1016/j.str.2012.01.014.

54. Crowell RL, Philipson L. 1971. Specific alterations of coxsackievirus B3 eluted from HeLa cells. J Virol 8:509–515.

55. Fricks CE, Hogle JM. 1990. Cell-induced conformational change in poliovirus: externalization of the amino terminus of VP1 is responsible for liposome binding. J Virol 64:1934–1945.

56. Carson SD. 2014. Kinetic models for receptor-catalyzed conversion of coxsackievirus B3 to A-particles. J Virol 88:11568–11575. http://dx.doi.org/10.1128/JVI.01790-14.

57. Organtini LJ, Makhov AM, Conway JF, Hafenstein S, Carson SD. 2014. Kinetic and structural analysis of coxsackievirus B3 receptor interactions and formation of the A-particle. J Virol 88:5755–5765. http://dx.doi.org/10.1128/JVI.00299-14.

58. Curry S, Chow M, Hogle JM. 1996. The poliovirus 135S particle is infectious. J Virol 70:7125–7131.

59. Butan C, Filman DJ, Hogle JM. 2014. Cryo-electron microscopy reconstruction shows poliovirus 135S particles poised for membrane interaction and RNA release. J Virol 88:1758–1770. http://dx.doi.org/10.1128/JVI.01949-13.

60. Luca VC, AbiMansour J, Nelson CA, Fremont DH. 2012. Crystal structure of the Japanese encephalitis virus envelope protein. J Virol 86:2337–2346. http://dx.doi.org/10.1128/JVI.06072-11.

61. Pierson TC, Sánchez MD, Puffer BA, Ahmed AA, Geiss BJ, Valentine LE, Altamura LA, Diamond MS, Doms RW. 2006. A rapid and quantitative assay for measuring antibody-mediated neutralization of West Nile virus infection. Virology 346:53–65. http://dx.doi.org/10.1016/j.virol.2005.10.030.

62. Mukherjee S, Lin TY, Dowd KA, Manhart CJ, Pierson TC. 2011. The infectivity of prM-containing partially mature West Nile virus does not require the activity of cellular furin-like proteases. J Virol 85:12067–12072. http://dx.doi.org/10.1128/JVI.05559-11.